Ac response to humidity and propane of sprayed Fe-Zn oxide films

A. Avila-García[a]*, M. García-Hipólito[b], and Y. Matsumoto-Kuwabara[a]
[a]*Sección de Electrónica del Estado Sólido, Departamento de Ingeniería Eléctrica, CINVESTAV del Instituto Politécnico Nacional, Apartado Postal 14-740, G.A. Madero 07360, D.F., México.*
**e-mail: aavila@cinvestav.mx*
[b]*Instituto de Investigaciones en Materiales, Universidad Nacional Autónoma de México, Apartado Postal 70-360, Coyoacán, 04510 México, D.F., México.*

Recibido el 29 de febrero de 2008; aceptado el 3 de julio de 2009

Iron-zinc oxide films with different Zn contents were ultrasonically sprayed on glass substrates and inter-digital gold electrodes were evaporated on them. Films were deposited from solutions containing 2, 10 and 30 at.% Zn. Hematite, amorphous and Franklinite structures resulted, respectively. They were assessed as humidity and propane detectors under alternating-current conditions for frequencies from 1 to 10^5 Hz and two temperatures: 30 and 250°C. Their impedances in dry air, humid air and humid air plus propane were determined from voltage measurements with a Lock-In amplifier. Sensitivity values to both humidity (53% RH.) and 189, 500 and 786 ppm of propane from the response of the real and imaginary parts of the impedance and also the total impedance were determined as functions of frequency. Maximum sensitivity for each case and the corresponding frequency are reported. The maximum sensitivity to humidity ranges from 24% up to 308%. In the case of propane, the maximum sensitivity ranges from 45% up to 711%. The largest sensitivity values correspond in all cases to the imaginary part of the impedance. From the dynamical response, the response and recovery times are determined, along with the concentration-dependence of the sensitivity. The sensing mechanisms are also discussed.

Keywords: Iron-zinc oxide films; ultrasonic spray pyrolysis; AC measurements; humidity and propane sensors.

Se depositaron peliculas de óxido de fierro con distintos contenidos de Zn sobre subestratos de vidrio y se les evaporaron electrodos interdigitados de oro. Se usaron soluciones conteniendo 2, 10 y 30% atómico de Zn. Resultaron películas con estructuras de hematita, amorfa y franklinita, respectivamente. Tales estructuras fueron probadas como sensores de humedad y propano bajo condiciones de corriente alterna para frecuencias entre 1 y 10^5 Hz y a dos temperaturas: 30 y 250°C. Se calcularon sus impedancias en aire seco, aire húmedo y aire húmedo más propano, mediante mediciones de voltaje con un amplificador Lock-In. Se determinaron los valores de sensibilidad a la humedad (53% HR) y a 189, 500 y 786 ppm de propano de las respuestas de la partes real e imaginaria de la impedancia y también de la impedancia total, como funciones de la frecuencia. Se reportan la máxima sensibilidad para cada caso y la frecuencia correspondiente. La sensibilidad máxima a la humedad está entre 24% y 308%. En el caso de propano, la sensibilidad va desde 45% hasta 711%. La mayor sensibilidad corresponde en todos los casos a la parte imaginaria de la impedancia. Se determinan los tiempos de respuesta y de recuperación de la respuesta dinámica, además de la dependencia de la sensibilidad con la concentración. Se comentan los mecanismos de sensado.

Descriptores: Películas de óxido de fierro-zinc; rocío químico ultrasónico; mediciones en CA; sensores de humedad y de propano.

PACS: 73.25.+i; 73.61.Le; 73.90.+f

1. Introduction

Some materials for gas sensors have been widely studied. For instance gas sensors based on Sn O_2 [1,2], ZnO [3,4], WO_3 [5,6] or Cr_2O_3 [7,8] have been described. In particular, iron oxide has also become an important material for this application [9,10]. In most of these studies, the DC response is reported and only a few researchers have provided results based on ac-measurements [11]. In this work, mixed iron-zinc oxide films with distinct zinc content are assessed as humidity and propane detectors. As a consequence of their different composition, these films also have different structures. Furthermore, not only the resistive response, but also the reactive one is determined. The corresponding ac measurements are carried out for variable frequency and two different temperatures. As a consequence of having the frequency as an extra variable for the electrical response, the possibility of enhancing sensitivity is stressed. Such sensitivity is defined in terms of the response of the real and the imaginary parts of the impedance (Z' and Z" respectively) and also the total impedance (Z), providing more alternatives for improvement.

2. Experimental details

The films were prepared by using the ultrasonic spray pyrolisis method starting with an aqueous (0.05M) solution of iron nitrate nonahydrate, combined with an appropriate amount of zinc acetate dihydrate to achieve the desired Zn/Fe ratio. Films from solutions with 2, 10 and 30 Zn at.% are discussed in this work. Depositions were performed during 5 minutes on glass substrates placed on a stainless steel plate heated to 450°C. The carrier gas (nitrogen) flow was 5.9 liters/min and the substrate placed about 1 cm below the nozzle. X-ray diffraction measurements were taken in order to find the composition and structure of each type of film. For the electrical measurements, interdigitated gold electrodes were evaporated throughout a metallic mask upon the free surface of the films. The area occupied by the contacts is about 9×9 mm^2

with a separation between adjacent fingers about 0.5 mm. The thickness of the contacts is about 1 μm. The a-c measurements for the electrical characterization were made with an SR830 Lock-In amplifier in a simple series circuit. The samples were placed within a controlled-temperature chamber where the atmosphere can also be changed by opening and closing the appropriate valves to control different gas flows. The equivalent circuit is depicted in Fig. 1. The voltage v_i is a sinusoidal signal whose frequency and amplitude can be controlled. The amplitude used was always 15 mV RMS. The alternating signal is internally provided by one of the Lock-In amplifier circuits. Z stands for the sample impedance, and C_c is an input coupling capacitance of known value that can be bypassed if DC coupling is desired. Finally, R_i and C_i are the resistance and capacitance at the input of the measuring circuit of the Lock-In amplifier. These last values can be determined experimentally. In our case, after connecting a known test resistance within the above-mentioned chamber, C_c, R_i and C_i turned out to be 0.1157 μF, $9.423 \times 10^6 \Omega$ and 150.8 pF, respectively. Hence, by knowing v_i and all the values of elements at the Lock-In input, the Z value can be calculated by measuring the complex voltage v. Since no DC offset voltage was applied to the sample, the gold contacts need to behave ohmic only within the 15 mV RMS around the zero bias operating point. The data acquisition is computer-controlled at different temperatures and frequencies. With this experimental system, either time, temperature or frequency scans can be performed.

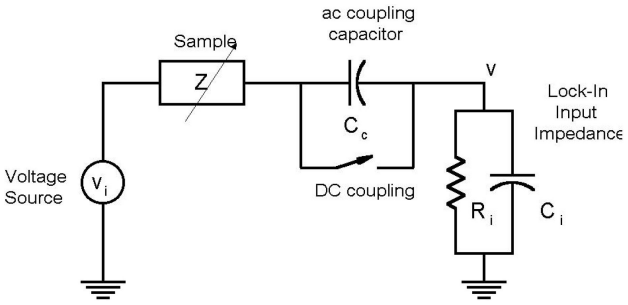

FIGURE 1. Equivalent circuit of the ac measurement system. v_i is a sinusoidal voltage. C_c, R_i and C_i belong to the input circuit of the Lock-In amplifier. The dashed line denotes bypassing of the input coupling capacitor when DC coupling is used.

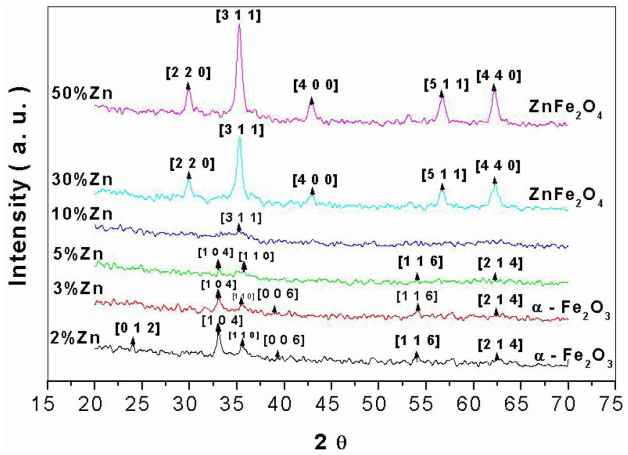

FIGURE 2. X-ray diffraction spectra of films deposited from solutions with different Zn content as indicated. It is clear that hematite (α-Fe_2O_3) dominates the film structure for Zn percentages below 5%, but it is highly disordered for this last value. On the other hand, for 10% the structure is also highly disordered, but starts to be mainly of Franklinite type ($ZnFe_2O_4$), which dominates for higher Zn percentages.

As mentioned above, films from solutions containing 2, 10, and 30 atomic% Zn were prepared. They were previously seen to have a hematite (2%), amorphous-like (10%) and franklinite (30%) structure [12,13] as it is shown in Fig. 2. Hence, films with different structures were assessed as humidity and propane sensors.

Frequency scans between 1 and 10^5 Hz with 15 points per frequency decade at two different temperatures, 30 and 250°C and under controlled atmospheres were performed. Three different atmospheres were used to interact with the surface of the samples. The first is synthetic dry air (D) consisting of 80% nitrogen and 20% oxygen. The second consists of the former dry air that is led through a bubbler to produce air with $\sim$ 53% relative humidity (H). The third one is humid air added with an appropriate flow of 1000 ppm propane in air to get the desired gas ratio (HP). A total flow of about 225 ml/min was maintained in all experiments. The gas outlet of the chamber is open to the atmosphere. Hence, pressures inside and outside the chamber are considered to be practically constant atmospheric pressure in all measurements. For this reason, this is practically independent of the pressure at the chamber gas inlet; still this is also kept constant in time by the usual pressure regulators used for the gas containers.

3. Results

3.1. Frequency scans

Although the measurement signal is small and no DC offset was applied, DC voltage measurements of the samples, between –1 V and +1 V, were performed to assess the ohmicity of the gold contacts. These I-V plots are depicted in Fig. 3. The worst case is seen to be that of the hematite sample, with some non-linearity of the current. Nevertheless, this is far from 0 V, where the ac measurements are performed. The other two I-V characteristics are much more linear in the whole voltage range shown.

As a result of frequency measurements, several plots can be built for each sample at a given temperature and atmosphere. This is illustrated in Fig. 4 in a similar way to that suggested by Macdonald *et al.* [14]. In this figure, the results corresponding to the sample with 2% Zn in dry air (D), humid air (H) and humid air plus 500 ppm propane (HP) at 30°C are shown. The projections of the three-dimensional path (not shown for clearness) defined by Z" as a function of

both frequency and Z' are depicted on the coordinate planes. Two of these projections describe the frequency dependence of the real and imaginary parts of the impedance Z. The third one is the so-called impedance plot describing the dependence of the imaginary part as a function of the real part of the impedance. In this way, a complete description is provided for any sample. Similar plots for all samples (2, 10 and 30% Zn) under three environments (D, H and HP) and two temperatures (30 and 250°C) can be obtained, but for the sake of simplicity they are not all shown. In this figure a strong effect of humidity can be observed upon Z' and Z". It consists of an appreciable decrease in both components for all the frequencies. On the other hand propane tends to reverse such a decrease, although not totally.

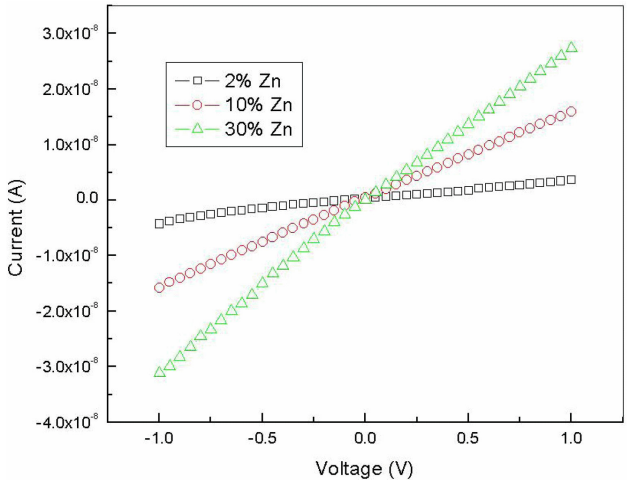

FIGURE 3. Direct Current I-V plots from –1 V up to +1 V for the distinct samples. Only the line of the hematite sample bears clear non-linear behavior. Nevertheless, it is far from the origin, where the small sinusoidal signal is applied for the measurement.

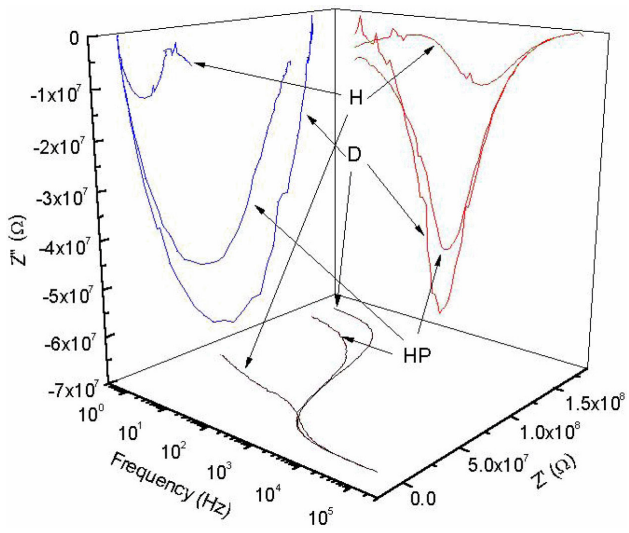

FIGURE 4. Projections of the three-dimensional paths defined by Z" vs. both, Z' and the measurement frequency, according to Macdonald et al. In this case, results for the sample with 2% Zn at 30°C are shown. In each coordinate plane, three projections are plotted: one for the dry air response (D), the second for the humid air atmosphere (H) and the third one for the humid air plus propane (HP) response. As projections on the coordinate planes, the real and imaginary parts of the impedance are shown as a function of frequency in the horizontal and right-side vertical planes. Besides, the imaginary vs. the real part is also plotted in the left-side vertical plane.

An equivalent circuit can be ascribed to the sample, depending on the frequency behavior of the impedance. Even without explicitly finding the magnitude of the elements in the equivalent circuit, their approximate size can be noticed. For instance, by observing the real part axis in Fig. 4, a rough idea of the resistive elements can be obtained. In the range of low frequencies, a large decrease in resistive elements, from about $1.5 \times 10^8\ \Omega$ to less than $5 \times 10^7 \Omega$ is seen in Fig. 4 after exposing the sample to humidity. Then, after exposing the same sample to propane, an increase in this resistance up to $\sim 1.3 \times 10^8 \Omega$ is seen. These changes reflect an important effect of both humidity and propane on the film properties. In the same way, the imaginary part is also importantly affected under the same circumstances.

3.2. Sensitivity

In order to give a quantitative measurement of the effect of both humidity and propane on our samples, the following expression is used here to define the sensitivities (in percentage):

$$S_{H,P}(X) = \left| \frac{X_{H,HP}}{X_{D,H}} - -1 \right| * 100. \qquad (1)$$

In this expression X can be either Z', Z" or |Z|. From Eq. (1), the frequency dependence of any of the above mentioned sensitivities can be obtained. The subscript D in the denominator is used with H in the numerator to calculate the sensitivity to humidity, and H in the denominator with HP in the numerator make it possible to determine the sensitivity to propane within the humid atmosphere.

In Fig. 5 the sensitivities to 53% R.H. and 500 ppm of propane, calculated with formula (1) are shown in the case of the hematite film (2% Zn). The amplitude of the measurement signal was 15 mV RMS. These plots were calculated on the basis of the real part response (squared symbols), imaginary part response (circles) and total impedance response (triangles). Both sensitivities, to humidity S_H and to propane S_P, are plotted against frequency. Different behaviors with frequency and magnitudes of sensitivity can be observed in these plots. It is seen that sensitivities at 30°C reach larger values than those occurring at 250°C. It can also be noticed that the maximum values of reactive responses are larger than resistive ones. For instance, regarding humidity in Fig. 5a S_H(Z') reaches a maximum value of 74% at 34 Hz while S_H(Z") is 91% at 100 Hz. Regarding the case of propane in Fig 5b, S_P(Z') is 219% at 34 Hz while S_P(Z") becomes 711% at 100 Hz. These results correspond to 30°C. It is noticeable that lower sensitivities of about 10% are obtained for

TABLE I.

Sample	T (°C)	Humidity			Propane		
		Response Type	S_H (%)	Frequency (Hz)	Response Type	S_P (%)	Frequency (Hz)
2% Zn	30	Z”	91	100	Z”	711	100
	250	Z”	107	73564	Z”	99	73564
10% Zn	30	Z”	213	1≤f≤4	Z”	48	1≤f≤4
	250	Z”	74	46415	Z”	242	46415
30% Zn	30	Z”	308	1≤f≤10	Z”	475	1000
	250	Z”	24	63095	Z”	45	63095

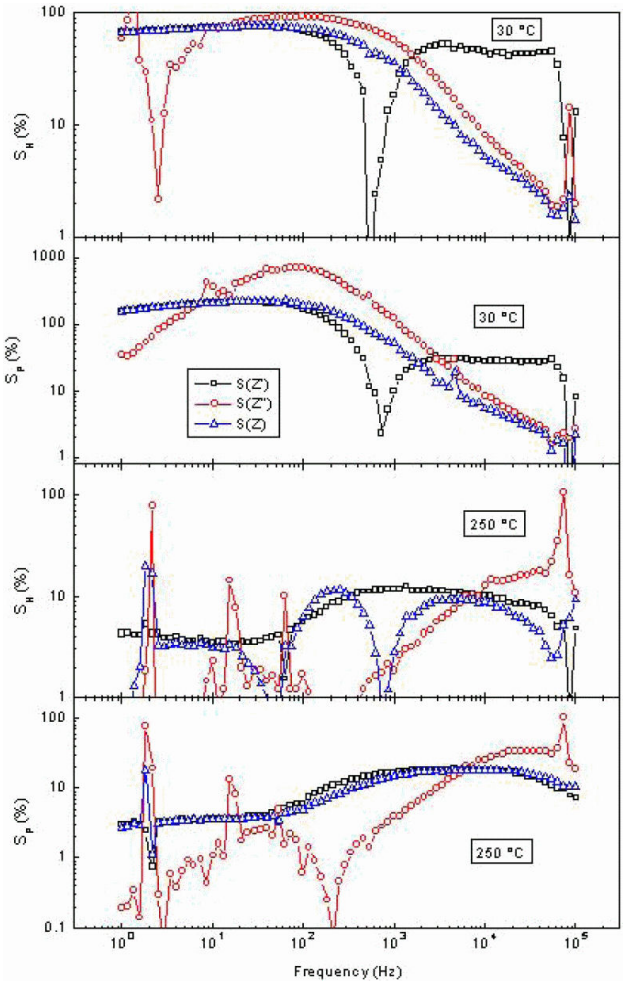

FIGURE 5. Sensitivities of the real (squared symbols), imaginary (circles) parts of and total impedance (triangles) as functions of the frequency. Results of the sample with 2% Zn at 30 °C and 250 °C are shown.

both humidity and propane at 250°C. The exceptions are near frequencies where $S_{H,P}$(Z”) peaks near 100%. Near these frequencies, more detailed measurements are needed. However, in the range from approximately 10 KHz to 50 KHz, both S_H(Z”) and S_P(Z”) reach around 20%.

As noted above, some of our results present curves peaked upwards. This normally happens in the imaginary part response. These peaks occur at the frequencies where the curve of the denominator in Eq. (1) becomes closer to zero. It is clear that frequency regions around such peaks allow large sensitivities to be obtained. In this figure (Fig. 5c) a frequency range where oscillatory imaginary sensitivities are of the order of 1% or less can be seen. The oscillation is the result of noise effects. Fortunately, this oscillation in our results appears mostly for sensitivities lower than 10%, then becoming of less practical importance.

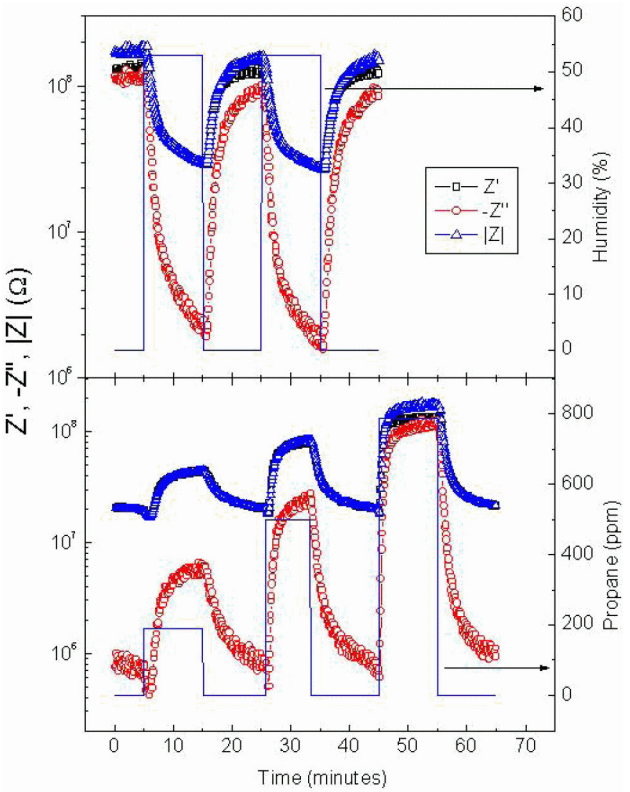

FIGURE 6. Dynamical responses of the hematite film (2% Zn) at 30°C measured with a 100 Hz, 30 mV sinusoidal voltage. In the upper graph the response of the total impedance and its real and negative imaginary parts are depicted, along with the humidity profile applied. The lower graph depicts the similar responses to different concentrations of propane as indicated by the continuous line, added to humid air.

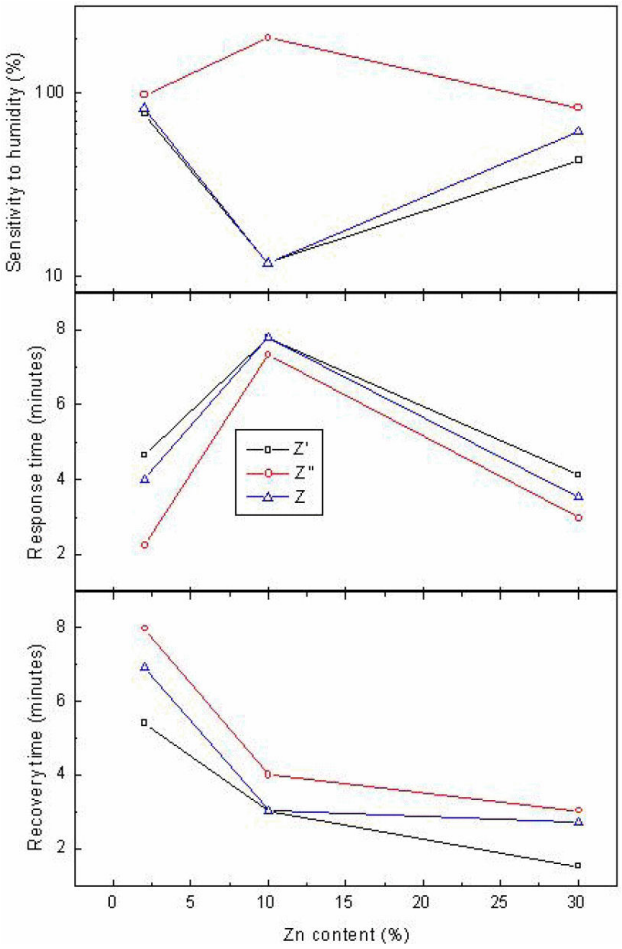

FIGURE 7. Results obtained for Z', Z" and |Z| from the analysis of the dynamical response to humidity, as functions of the Zn content. The upper graph illustrates the dependence of the sensitivity on the Zn content. The middle one contains the response time and the lower the recovery time.

The greatest sensitivities obtained with the different samples at the two temperatures studied are included in Table I, confirming that all of them correspond to the response of the imaginary part of the impedance (Z"). From this table it turns out that the best film to sense humidity is that with the Franklinite structure (30% Zn). The corresponding conditions of the measurement are 30°C and a frequency range from 1 to 10 Hz. On the other hand, 500 ppm of propane are best detected at 30°C and at a frequency of 100 Hz by the film with the hematite structure (2% Zn). However, all sensitivities in Table I are reasonable, providing several possibilities to detect either humidity or propane. Hence, an important feature of the ac-measurement method, thus stressing its relevance, is that maxima under different conditions are obtained at different frequencies.

3.3. Dynamical behavior

In order to illustrate the time-dependent response of Z', Z" and |Z| to humidity and propane, this last in different concentrations, we show the hematite (2% Zn) results in Fig. 6. They were obtained at 30°C and 100 Hz with a small signal of 30 mV amplitude. As indicated in the upper graph, a constant relative humidity of 53% was applied to the sample along 10 minute intervals, allowing for recovery also during 10 minutes each time. Two cycles of this type are shown. In the lower graph three concentrations of propane are applied during 10 minutes to the sample immersed in humid air: 189, 500 and 786 ppm and also 10 minute intervals are allowed for recovery. The three response types considered here are plotted in both graphs. Once again the Z" response is clearly larger than the others. We considered the maximum change after applying either humidity or propane to calculate the associated sensitivity. The time needed to reach 90% of the total change along the corresponding interval is calculated to determine both the response and the recovery times. An analysis of the curves in Fig. 6 and the graphs corresponding to the other samples (that with 10% Zn was measured under 15 mV at 2 Hz and that with 30% Zn under 15 mV at 1 KHz) yielded the values related to humidity response shown in Fig. 7. In the upper graph the highest sensitivities to

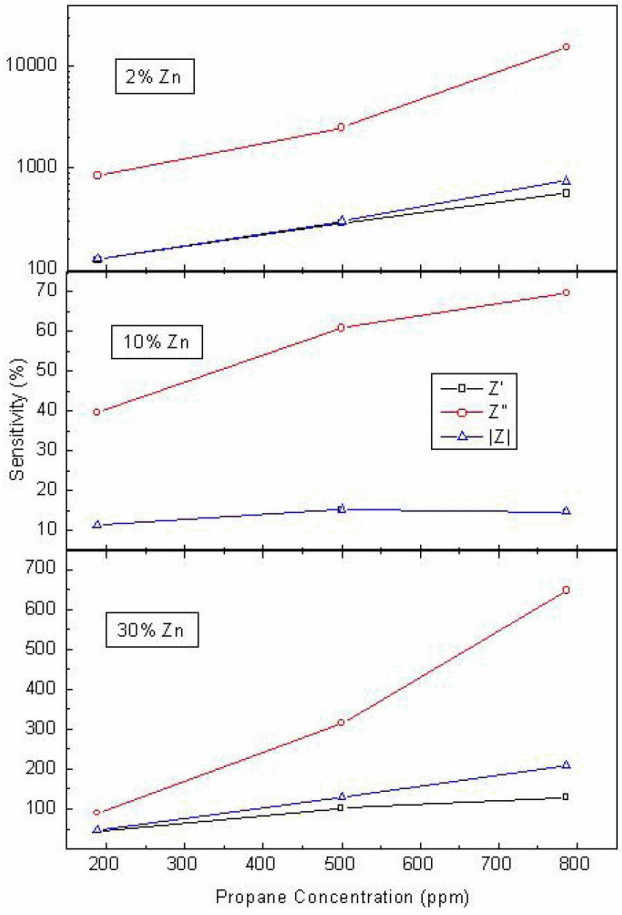

FIGURE 8. Sensitivity dependence of Z', Z" and |Z| on the propane concentration. In the upper graph, an exponential variation can be noticed for the case of the hematite sample. In the middle and lower graphs, the dependence is closely linear for the amorphous and the franklinite samples.

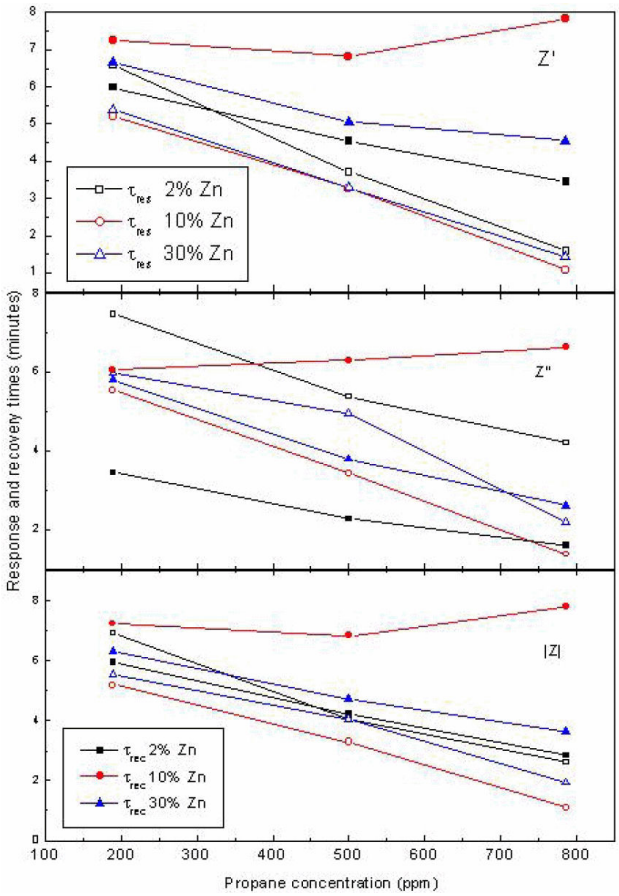

FIGURE 9. Behavior of the response and recovery times plotted as functions of the propane concentration. The variations of such times associated to Z', Z" and |Z| of the different samples are described in the upper, middle and lower graphs, respectively. The squares correspond to the hematite sample, the circles to the amorphous one and the triangles to the franklinite sample. Empty symbols describe the response times and the full symbols the recovery times.

humidity once more correspond to the imaginary part of the impedance, the largest ($\sim$ 200%) being that corresponding to the amorphous-like sample (10% Zn). In the middle graph the response times are the longest for the amorphous-like sample, between 7 and 8 minutes, but for the other samples it is less than 5 minutes, being the shortest that for the hematite sample (2% Zn), near 2 minutes. In the lower graph the longest recovery times correspond to the hematite sample, between 5 and 8 minutes, and the shortest to the franklinite sample, about 3 minutes or lower.

In Fig. 8 the sensitivity to propane of the three types of response are plotted for the different samples at 30°C as a function of the propane concentration. In the upper graph the responses of the hematite sample are seen to behave exponentially in the range of concentration involved. Instead, the responses of the disordered and franklinite samples are seen to vary linearly with concentration. The corresponding behaviors at 250°C are found to be reversed with respect to those mentioned above. The greatest sensitivities to propane correspond mostly to the hematite sample, only that of Z" being similar to the franklinite sample. The lowest are those of the disordered sample. The response of the imaginary part Z" turns out to be the highest in all cases. Since Z" sensitivity shows a capacitive behavior, it is related to fixed-charge exchange processes between the film and the test gas. In our samples this effect turns out to be more important than those which change the population of mobile charges that contribute to the conductivity process.

Times associated with the response and recovery processes of the films are plotted in Fig. 9 as functions of the propane concentration. The empty symbols correspond to the response times, and the full symbols to the recovery times. It is observed that most of the behaviors are decreasing. Furthermore, most of them are nearly linearly decreasing. The only exceptional case corresponds to the recovery time of the disordered sample and has a global increasing trend with propane concentration. This means that the recovery time of both Z' and Z" becomes the longest for 786 ppm of propane. Also, the response time of the same sample is the shortest for both Z' and Z". It seems that disorder in the film structure produces fast adsorption and slow desorption processes at 786 ppm. The shortest response times of the real part Z' are due to the disordered and franklinite samples, decreasing from about 5.3 minutes to 1.5 minutes. The disordered sample exhibits the shortest Z" response times in the range from $\sim$5.5 minutes to $\sim$1.5 minutes. The shortest recovery times belong to the hematite sample for both Z' and Z", with those for Z" being better.

Our experimental results at 30°C after exposing to humidity films with the three types of structure mentioned in this work yield a decrease in resistance. At this low temperature it is generally assumed that proton drift is the mechanism which produces these changes in the different materials studied here [10]. As propane is added, its reaction with OH^- radicals leads to intermediate $C_3H_7O^-$ species, which in turn trap $H^+$to form propanol. Then the ionic conductivity is decreased. This process explains the increase in resistance observed at low frequencies during the measurements for the three types of samples.

At higher temperatures (250°C in our case), humidity is able to alter the status of oxygen at the surface, including both molecular and ionic species [15]. However, we observed a decrease in resistance in the cases of all the three types of samples: hematite (2% Zn), amorphous-like (10% Zn) and franklinite (30% Zn). This would not happen if electronic processes dominated the conductivity, since the hematite sample is expected to be a p-type semiconductor, while franklinite is n-type [16-18]. Hence, we assume that proton drift still dominates the conductivity. This is consistent with the increase in resistance produced by adding propane.

4. Conclusion

Iron-zinc oxide films with 2, 10 and 30 at.% Zn possessing different structures (hematite, amorphous and Franklinite, respectively) were prepared on glass substrates at 450°C by ultrasonic spray pyrolisis from aqueous solution. They were assessed as humidity (53% R.H.) and propane (189, 500 and 786 ppm) sensors at 30 and 250°C. Their response to a sinusoidal alternating voltage signal was measured as a function of the frequency. Sensitivity values for the response of the real and imaginary parts of the impedance and also of the total impedance were determined. The greatest sensitivities for both humidity and propane were achieved from the response of the imaginary part of the impedance. Sensitivities to humidity and propane as large as ∼308 and ∼711%, respectively, are obtained from these cases. These figures correspond to the Franklinite-type (30% Zn) sample at a low temperature (30°C) and to the hematite sample (2% Zn) at 30°C, respectively. If a small effect of the humidity is desired to detect propane, namely at 250°C, then the best sensitivity (242%) is provided by the amorphous-like (10% Zn) sample. In general, good maximum sensitivities at both temperatures are achieved by all the samples studied. In the case of our samples, the sensitivity of the total impedance response is not as relevant as that of the imaginary part for most cases. In our view, it is possible to adequately choose a type of sample and temperature according to a desired work frequency. Regarding humidity, Z" of the disordered sample provides the highest sensitivity; Z" of the hematite film yields the fastest response; Z' of the franklinite film is the fastest to desorb water. With respect to propane, the highest sensitivity results from the response of Z" of the hematite film; Z' of the three samples behaves linearly with the propane concentration, but Z" behaves exponentially. The sensing mechanism of water at both temperatures of this work is involved with its decomposition at the surface to produce and adsorb H^+ and OH^- radicals. Thus, protons contribute to the ionic conductivity of the films. Under the presence of propane, such proton population is decreased, thus increasing the resistance of the films.

Acknowledgements

Help with the sample preparation is gratefully acknowledged to M. Sc. Carlos Torres Frausto and Miss Enriqueta Aguilar Valencia. Also, help with drawing of Fig. 1 is acknowledged to M. Sc. Gaspar Casados.

1. G. Heiland, *Sensors and Actuators* **2** (1981) 343.
2. Yu-De Wang, Chun-Lai Ma, Xing-Hui Wu, Wiao-Dan Sun, and Heng-De Li, *Talanta* **57** (2002) 875.
3. B.L. Zhu, C.S. Xie, W.Y. Wang, K.J. Huang, and J.H. Hu, *Materials Letters* **58** (2004) 624.
4. V.R. Shinde, T.P. Gujar, C.D. Lokhande, R.S. Mane, and Sung-Hwan Han, *Materials Science and Engineering: B* **137** (2007) 119.
5. Jun Tamaki, Atsushi Hayashi, Yoshifumi Yamamoto, and Masao Matsuoka, *Sensors and Actuators B: Chemical* **95** (2003) 111.
6. V. Khatko *et al.*, *Sensors and Actuators B, Chemical* **111-112** (2005) 45.
7. B.K. Miremadi, R.C. Singh, Z. Chen, S. Roy Morrison, and K. Colbow, *Sensors and Actuators B: Chemical* **21** (1994) 1.
8. Jing Du, Yiquan Wu, and Kwang-Leong Choy, *Thin Solid Films* **497** (2006) 42.
9. Wan-Young Chung and Duk-Dong Lee, *Thin Solid Films* **200** (1991) 329.
10. G. Neri, A. Bonavita, S. Galvagno, N. Donato, and A. Caddemi, *Sensors and Actuators B, Chemical* **111-112** (2005) 71.
11. Udo Weimar and Wolfgang Göpel, *Sensors and Actuators B, Chemical* **26-27** (1995) 13.
12. C. Torres Frausto, M.Sc. Thesis, Sección de Electrónica del Estado Sólido, Dep. de Ingeniería Eléctrica, CINVESTAV del I.P.N., México, D.F., November 2005.
13. C. Torres Frausto and A. Avila García, Proceedings of the 2004 1^{st} International Conference on Electrical and Electronics Engineering, Acapulco, Guerrero, México, September, 2004, 282.
14. J.R. Macdonald, J. Schoonman, and A.P. Lehnen, *Solid State Ionics* **5** (1981) 137.
15. T. Sahm, A. Gurlo, N B?rsan, and U. Weimar, *Sensors and Actuators B* **118** (2006) 78.
16. D.M. Smyth, *The defect chemistry of metal oxides* (Oxford University Press, New York, 2000).
17. C. Nai-Sheng, Y. Xiao-Juan, L. Er-Sheng, and H. Jin-Ling, *Sensors and Actuators B* **66** (2000) 178.
18. M. Pelino, C. Cantalini, H.T. Sun, and M. Faccio, *Sensors and Actuators B* **46** (1998) 186.